energy playing a major role in the transfer kinetics. This ZnO experiment basically demonstrates that, with a correct alignment of energy levels, electron transfer can take place by direct tunneling to solvated ions within about 15 Å of the surface. The reduced reaction product is born fully solvated. We suggest that an initial Raman spectrum under these conditions would be essentially that of the aqueous species.

In our experiments we observe reaction products with a shortest delay time of $\sim 5 \times 10^{-9}$ s. In aqueous solution a small, free inorganic ion could diffuse ~40 Å in this time. However, in our pH 10 CdS and TiO_2 experiments, the crystallite surfaces have a net negative charge due to OH^- specific adsorption. Both reactant MV^{2+} and product MV^+ are electrostatically attracted to the surface. In the CdS experiment, the observation that the product MV^+ shows Langmuir isotherm saturation implies (a) that the MV^{2+} surface sites available for reduction are filled before the light pulse excites the crystallite and (b) possible MV^+ desorption and subsequent adsorption of another MV^{2+} from further out in the double layer is slow with respect to $\sim 5 \times 10^{-9}$ s. In this sense the MV^+ remains "adsorbed" as its Raman spectrum is generated. Some angstrom-scale movement and resolvation of the MV^+ after formation is certainly possible.

In a similar fashion, the $C_{14}MV^+$ signal in the TiO_2 experiments is reported to be independent of initial $C_{14}MV^{2+}$ concentration and to show no kinetic rise time.[9] The surface must be saturated with $C_{14}MV^{2+}$. The hydrophobic C_{14} chain presumably anchors MV^{2+} and reduced MV^+ with respect to the TiO_2 surface and its supporting copolymer. The MV^{2+} moiety appears to retain its solvation sheath.

The SERS effect on metal surfaces is characterized by (a) a $\sim 10^6$ enhancement in cross section and (b) a substantial shift in Raman frequencies for chemisorbed molecules in the first layer. In reactions 1-4, we see no frequency shift. There is also no evidence for a large cross-section enhancement for any species on the surface, although we cannot make a quantitative statement here. This absence of SERS is consistent with (a) the apparent absence of strong chemisorption coupling the molecule to the crystallite delocalized electrons and (b) the expected absence of enhanced electromagnetic fields near these crystallites. The intensity of the local field[36] near a small material sphere (in vacuum) is proportional to

$$I_{loc} \propto \left[\frac{\epsilon - 1}{\epsilon + 2}\right]^2 \quad (7)$$

where ϵ is the complex dielectric coefficient. For Ag near 380 nm, Re $\epsilon \simeq -2$ and Im $\epsilon < 1$, yielding a large I_{loc}. However, these conditions are not satisfied by bulk CdS at 395 nm[37] and any semiconductor at wavelengths below the band gap.

Conclusions

The initial Raman spectra provide strong confirmation that the elementary surface electron-transfer processes 1-4 occur when colloidal crystallites are irradiated above their band gaps.

The Langmuir isotherm behavior coupled with the absence of perceptible distortion in the Raman spectra suggests but does not rigorously prove, that charge transfer occurs to electrostatically adsorbed reactants that retain their first water solvation layers. The strong distortion characteristic of SERS spectra is not observed.

We stress that we have studied simple e^- transfer involving ionic species. Solvation energies are highest for ionic species in water. It is possible that with neutral precursors and/or in less polar solvents, a stronger interaction with the surface will be found. There are also numerous more complex electrode surface reactions that are exothermic, yet kinetically very slow. In these cases it may be that "specific adsorption" at special sites is necessary for reaction.

Acknowledgment. We thank Prof. M. Grätzel for discussion, a preprint of ref 9, and a gift of $C_{14}MV^{2+}$. S. Nakahara collaborated on the TEM studies, and B. Miller provided valuable comments on an earlier verison of this manuscript.

Registry No. TiO_2, 13463-67-7; CdS, 1306-23-6; MV^{2+}, 4685-14-7; SCN^-, 302-04-5; $C_{14}MV^{2+}$, 79039-57-9; $(SCN)_2^-$, 34504-17-1; MV^+, 25239-55-8; $C_{14}MV^+$, 88376-68-5.

(36) Gersten, J.; Nitzan, A. *J. Chem. Phys.* **1980**, *73*, 3023, eq 5.9.
(37) Cook, R. K.; Christy, R. W. *J. Appl. Phys.* **1980**, *51*, 668.

Kinetics of the Chemical and Electrochemical, Reversible Oxidation of Bis(dithiooxalato-*S*,*S*′)cuprate(II), $[Cu(Dto)_2]^{2-}$. A Facile, Light-Activated, Intramolecular Electron Transfer and Cleavage of the C–C Bond in the Coordinated Dto Ligands in the $[Cu(Dto)_2]^-$ Anion

T. Imamura, M. Ryan,[1a] G. Gordon,*[1b] and D. Coucouvanis*[1c]

Contribution from the Departments of Chemistry, University of Iowa, Iowa City, Iowa 52242, and Miami University, Oxford, Ohio 45056. *Received April 4, 1983*

Abstract: The rates of reaction of bis(dithiooxalato-*S*,*S*′)cuprate(II), $[Cu(Dto)_2]^{2-}$, with Cu(II) and Fe(III) have been measured and the corresponding rate constants and activation parameters are reported. In addition, the electrochemistry of this complex and of the oxidation product $[Cu(Dto)_2]^-$ was studied in detail. The $[Cu(Dto)_2]^-$ anion undergoes a light-activated, intramolecular, Dto → Cu two-electron transfer with cleavage of the C–C bond in the Dto ligand and generation of gaseous SCO. Addition of triphenylphosphine to $[Cu(Dto)_2]^-$ in the presence or absence of light also results in intramolecular redox and cleavage of the C–C bond.

In a previous communication[2] we reported on the unusual, reversible, oxidative C–C bond cleavage of the coordinated dithiooxalate (Dto) ligand in the $[Cu(Dto)_2]^{2-}$ complex (I). This oxidation was effected chemically in dimethylformamide (DMF)

0002-7863/84/1506-0984$01.50/0

or CH_2Cl_2 by either Cu(II) or Fe(III) ions and resulted in the formation of a crystalline product that was formulated as a Cu(I) carbonyl sulfide complex, $[Cu(Dto)(SCO)_2]^-$, containing end-on S-coordinated SCO. This formulation was based on (a) a strong absorption band in the infrared spectrum at 2045 cm^{-1}, (b) the vigorous evolution of gaseous SCO following the addition of triphenylphosphine (PPh_3) to solutions of this compound, and (c) the isolation of crystalline salts of the $[Cu(Dto)(PPh_3)_2]^-$ anion from such solutions.

A recent structure determination of the oxidation product revealed that this compound contains two intact Dto ligands, and the anion can be best formulated as the $[Cu(Dto)_2]^-$ complex (II), which contains copper in the +3 formal oxidation state.

Further studies on salts of II indicated that the apparent cleavage of the C–C bond in one of the coordinated Dto ligands is light-induced and that the presence of the SCO absorption in the infrared spectrum is due to the effects of the visible-light component of the infrared light source.

A kinetic study of the oxidation of I was undertaken in an attempt to establish the rate law, determine activation parameters, and derive a possible mechanism for the oxidation process.

Experimental Section

Synthesis. The chemicals in this research were used as purchased. Reagent grade dichloromethane, CH_2Cl_2, was distilled[3] by using a 45-cm Vigreux column; the middle fraction was collected after refluxing over phosphorus pentoxide[4] for 12 h. The purified CH_2Cl_2 solvent was purged with dry nitrogen and was stored in the dark. Reagent grade tetrabutylammonium chloride, Bu_4NCl, was dried in a desiccator under vacuum for 100 h prior to use. Dichloromethane was chosen as the solvent for the kinetic studies due to the high stability of the complexes in this solvent.

The carbon, hydrogen, and nitrogen analyses were determined by the Microanalytical Services Lab at the University of Iowa, while the copper was determined by atomic absorption.[5]

Preparation of Compounds. Bis(benzyltriphenylphosphonium) Bis(dithiooxalato-*S*,*S*')cuprate(II), $(BzPh_3P)_2Cu(S_2C_2O_2)_2$. An amount of $BzPh_3PCl$, 3.88 g (10.0 mmol), was dissolved in 100 mL of water containing 0.65 g (5.0 mmol) of $CuCl_2 \cdot 2H_2O$. This solution was added with stirring to a solution of 2.0 g (10.0 mmol) of $K_2S_2C_2O_2$ in 100 mL of water. The green-yellow precipitate, which formed instantly, was filtered and allowed to dry in vacuo. This precipitate was dissolved in 150 mL of dimethylformamide, DMF, to give an intense green solution. Diethyl ether was added to the solution to incipient crystallization, and the solution was cooled to ca. 10 °C and allowed to stand for ca. 4 h. Brown, light-sensitive crystals formed and were isolated (3.0 g, 60% yield).

Anal. Calcd for $C_{54}H_{44}P_2S_4O_4Cu$: C, 64.20; H, 4.36; Cu, 6.29. Found: C, 64.38; H, 4.27; Cu, 6.25.

X-ray powder pattern spacings (Å): 11.63 (s), 8.90 (w), 7.33 (s), 6.76 (w), 6.27 (s), 5.83 (s), 5.05 (m), 3.97 (s), 3.45 (m), 3.32 (w).

Benzyltriphenylphosphonium Bis(dithiooxalato-*S*,*S*')cuprate(III)–Dichloromethane, $(BzPh_3P)Cu(S_2C_2O_2)_2 \cdot CH_2Cl_2$. All operations must be carried out in the dark. To a suspension of 2.0 g (2.0 mmol) of $(BzPh_3P)_2Cu(S_2C_2O_2)_2$ in 150 mL of dichloromethane, CH_2Cl_2, was added 0.75 g (2.8 mmol) of $FeCl_3 \cdot 6H_2O$ dissolved in 25 mL of acetone. The resulting solution was stirred for 5 min. This red solution was extracted with five 150-mL portions of water to remove the water-soluble salt byproducts. After the CH_2Cl_2 solution was dried with $CaSO_4$, 50 mL of pentane was added and the unreacted reagents were removed by filtration. To the filtrate a 3:1 pentane/ether mixture was added to incipient crystallization, and the mixture was allowed to stand in the dark. Red crystals formed and were isolated (1.1 g, 75% yield).

Anal. Calcd for $C_{30}H_{24}PS_4O_4Cl_2Cu$: C, 48.55; H, 3.24, Cu, 8.56. Found: C, 48.83; H, 3.26; Cu, 8.21.

Benzyltriphenylphosphonium (Dithiooxalato-*S*,*S*')bis(triphenylphosphine)cuprate(I), $(BzPh_3P)Cu(S_2C_2O_2)(PPh_3)_2$. An amount of $(BzPh_3P)Cu(S_2C_2O_2)_2 \cdot CH_2Cl_2$, 2.0 g (~3.0 mmol), was dissolved in 30 mL of CH_2Cl_2 and was added dropwise to a 100-mL CH_2Cl_2 solution containing 2.5 g (9.5 mmol) of triphenylphosphine, PPh_3. Immediate evolution of SCO occurs. The resulting orange solution was then diluted with *n*-pentane to incipient crystallization and the mixture was allowed to stand. An orange crystalline solid formed and was isolated. The crude product was recrystallized from an acetone/pentane mixture.

Anal. Calcd for $C_{63}H_{52}P_3S_2O_2Cu$: C, 71.32; H, 5.25; Cu, 5.99. Found: C, 70.90; H, 4.95; Cu, 6.10.

Bis(18-crown-6-potassium) Bis(dithiooxalato-*S*,*S*')cuprate(II), $(18\text{-crown-6})_2K_2Cu(S_2C_2O_2)_2$. To a solution of 1.0 g (5.05 mmol) of $K_2S_2C_2O_2$ in 50 mL of distilled water was added with stirring a solution of 430 mg (2.5 mmol) of $CuCl_2 \cdot H_2O$ in 50 mL of distilled water. The dark green solution of the $K_2Cu(S_2C_2O_2)_2$ complex that was obtained was extracted with a solution of 18-crown-6-ether, 1.3 g (5.06 mmol) in 50 mL of CH_2Cl_2. The CH_2Cl_2 phase assumed a dark green coloration and was isolated from the aqueous phase by filtration through phase-separating (silicone treated) filter paper.

The product was obtained as a dark green powder upon the addition of ether to the CH_2Cl_2 solution. The crude product was recrystallized from DMF upon the addition of ether to incipient crystallization and cooling.

Other salts of the various copper complexes were prepared by substituting $BzPh_3P^+$ with other cations in the synthetic procedures. All of the complexes were soluble in organic solvents. The Cu–Dto complexes are unstable in ethanol or dimethylformamide solutions even when the solvents were distilled repeatedly over I_2 with MgO or CaO and purged with dinitrogen gas. The $[Cu(S_2C_2O_2)_2]^-$ complex is relatively stable in CH_3CN which was freshly distilled over P_2O_5, showing about 15% decomposition per hour.

Physical Methods. A Varian A60 NMR spectrometer was used to determine the concentration of water present in the Bu_4NCl–CH_2Cl_2 solutions. The electronic spectra were recorded on a Cary 14 spectrophotometer. A Perkin-Elmer Model 421 recording IR spectrometer was used to determine the absence of water and purity of the complexes. The electrochemical experiments were performed by using a Princeton Applied Research Corp. (PARC) Model 173/176 instrument. The reference electrode was a saturated calomel electrode with a nonaqueous salt bridge (PARC Model M174). The working and auxiliary electrodes were a platinum bead and a platinum wire, respectively. Positive-feedback resistance compensation was used when appropriate. All solutions were deaerated with argon.

Kinetic Studies. All solutions were prepared immediately prior to use, in the dark under an atmosphere of prepurified nitrogen that was free from oxygen and water. The kinetic studies were carried out at the appropriate temperatures ±0.5 °C by using a Durrum stopped-flow spectrophotometer equipped with a Teflon cell with a path length of 2 cm. The volume of the solution that flowed through the cell in each experiment was adjusted to be at least 0.68 mL to ensure that all of the reactant solution in the cell came directly from the drive syringes,[6] where temperature control is most effective. For the reactions, the changes in absorbance were photographed directly from the storage screen of the oscilloscope. All kinetic experiments were carried out in the dark. In the study of the reaction of the dithiooxalate complex I with iron(III) or copper(II), the Bu_4NCl powder (white colored) was dried in a desiccator under vacuum for 5 days and was used to adjust the total concentration of ionic species at 0.01 M. The concentration of H_2O was measured by an NMR technique and for a 0.1 M solution of Bu_4NCl was shown to be less than 3×10^{-3} M. No effect was noted on the calculated rate constants.

Results

Synthesis and Characterization. The synthesis of the $[Cu(Dto)_2]^{2-}$ anion (I) from K_2Dto and $CuCl_2$ proceeds by a straightforward metathesis reaction only when the $CuCl_2$ solution is added to the solution of the ligand. Addition in the reverse order always results in a considerable amount of decomposition because of the oxidation of I by excess $CuCl_2$. Chemical oxidation of solutions of the Ph_4As^+ or $BzPh_3P^+$ salts of I in DMF or CH_2Cl_2 by $CuCl_2 \cdot 2H_2O$ or anhydrous $FeCl_3$, respectively, gave rise to the red, diamagnetic $[Cu(Dto)_2]^-$ anion (II), which is isolated in crystalline salts of various counterions. The infrared spectra of these light-sensitive compounds revealed the presence of S-coordinated dithiooxalate ligand ($\nu_{C=O}$ at 1640 and 1590 cm^{-1}) and a new strong band at 2055 cm^{-1}. Addition of PPh_3 to CH_2Cl_2 solutions of these compounds led to a vigorous evolution of gas. The infrared spectrum ($\nu_{C=O}$ 2064 cm^{-1}) and mass spectrum of this gas were those of gaseous SCO. The isolation of crystalline

(1) (a) On leave from the Department of Chemistry, Marquette University, Milwaukee, Wisconsin (July 1981 to July 1982). (b) Department of Chemistry, Miami University. (c) Present address: Department of Chemistry, The University of Michigan, Ann Arbor, Michigan 48109.

(2) Coucouvanis, D. *J. Am. Chem. Soc.* **1971**, *93*, 1786.

(3) Weissberger, A., Ed. "Techniques of Organic Chemistry", 2nd ed.; Interscience: New York, 1955; Vol. III.

(4) Vaugh, J. W. "The Chemistry of Non-Aquo Solvents"; Academic Press: New York, 1967.

(5) Leitheiser, M. Ph.D. Thesis, 1974, The University of Iowa, Iowa City, IA.

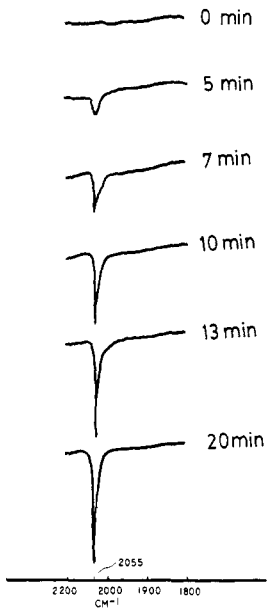

Figure 1. Intramolecular electron transfer and cleavage of the C–C bond of the Dto ligand in the $[Cu(Dto)_2]^-$ anion as a function of exposure time to the infrared light source.

Table I. Absorption Maxima and Molar Extinction Coefficients

copper complex	mol wt	ϵ, M^{-1} cm^{-1}
$(Bu_4N)_2Cu(Dto)_2$	788.77	$\epsilon_{400} = 11\,400$
$(BzPh_3P)_2Cu(Dto)_2$	1010.63	$\epsilon_{407} = 9130$
$(Ph_4P)_2Cu(Dto)_2$	982.57	$\epsilon_{383} = 11\,000$
$(EtPh_3P)_2Cu(Dto)_2$	887.55	$\epsilon_{405} = 8490$
$(Bu_4N)Cu(Dto)_2$	546.30	$\epsilon_{530} = 614$, $\epsilon_{380} = 20\,000$
$(BzPh_3P)Cu(Dto)_2$	657.23	$\epsilon_{530} = 758$, $\epsilon_{382} = 22\,300$

salts of the $[Cu(Dto)(PPh_3)_2]^-$ anion from the same reaction in good yields was as expected for the reaction

$$[Cu(Dto)(COS)_2]^- + 2PPh_3 \rightarrow [Cu(Dto)(PPh_3)_2]^- + 2COS$$

A recent crystallographic study of the light-sensitive[7] "[Cu(Dto)$(SCO)_2$(PNP)]" salt revealed that the planar anion contained two intact Dto ligands and was the monoanionic four-coordinate Cu(III) complex $[Cu(Dto)_2]^-$ (II). The crystallographic results prompted us to reexamine the physical and chemical properties of this complex. The first rapid scan in the narrow infrared region between 2020 and 2060 cm^{-1} showed no evidence of absorption at 2055 cm^{-1}. However, following repetitive scans over the same region, a band appeared at 2055 cm^{-1} that increased in intensity as a function of exposure time to the infrared light source[8] (Figure 1) and reached a maximum intensity in ca. $^1/_2$ h. It appears therefore that light, including the visible-light component of the filament infrared light source, promotes an intramolecular, two-electron, Dto → Cu transfer in II with cleavage of the C–C bond and generation of SCO. The evolution of SCO from solutions of II upon addition of Ph_3P suggests that Ph_3P interacts with II and promotes this intramolecular electron transfer. The occurrence of this reaction in either the presence of absence of light indicates that light activation is not necessary for the generation of SCO with Ph_3P present.

The slightly lower frequency of the "trapped" SCO in the irradiated crystalline salts of II may indicate weak, end-on S-coordination of the SCO molecules to Cu(I) in the photolysis product.

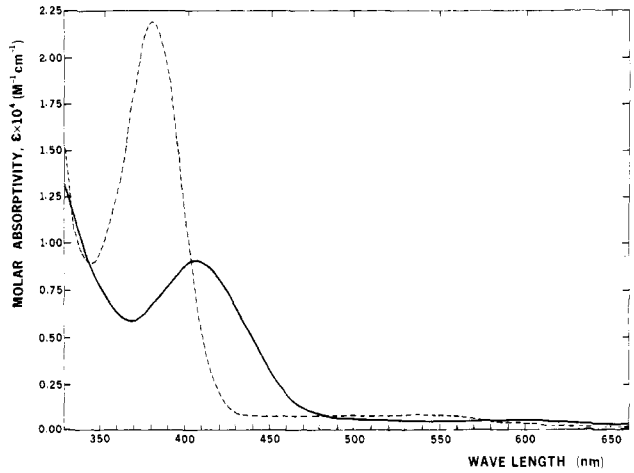

Figure 2. Electronic spectra of the Cu(II) and Cu(III) dithiooxalate complexes in CH_2Cl_2 at 25 °C: (—) $(BzPh_3P)_2Cu(Dto)_2$; (---) $(BzPh_3P)Cu(Dto)_2$.

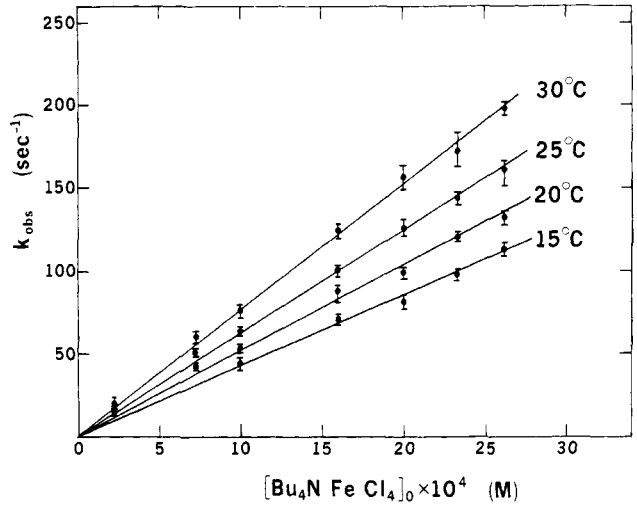

Figure 3. Rate constant for the $(Bu_4N)_2Cu(Dto)_2$–$(Bu_4N)FeCl_4$ reaction as a function of $[(Bu_4N)FeCl_4]$ in 0.1 M Bu_4NCl at various temperatures.

Kinetic Studies. The electronic structure and the spectral properties of the dithiooxalate complexes of nickel(II), palladium(II), and gold(III) have been reported previously.[9] The electronic absorption spectra for the $[Cu(Dto)_2]^{2-}$, I and $[Cu(Dto)_2]^-$ (II) complexes are shown in Figure 2. The absorption maxima and molar absorptivities of various salts of I and II in CH_2Cl_2 at 25 ± 0.2 °C are shown in Table I.

Major changes in the absorption spectra of complex I occur at 380, 430, 530, and 560 nm as a result of adding iron(III) or copper(II) solutions to complex I in solution. The changes at 430 and 530 nm were measured by using 2.54×10^{-4} M $[(Bu_4N)_2Cu(Dto)_2]_0$ and 4.36×10^{-3} M > $[(Bu_4N)FeCl_4]_0 \geq 0$ and 25 ± 0.5 °C in a 1-cm optical path length cell and show that the reaction proceeds in a 1:1 molar ratio.

Preliminary kinetic measurements were carried out for the reaction between $(Ph_4P)_2Cu(Dto)_2$ and $(Bu_4N)FeCl_4$. The changes in absorbance at 470, 530, and 620 nm were followed by mixing 10^{-4} M solutions at room temperature. The reaction proceeded rapidly and increase (530 nm) or decrease (470, 620 nm) of absorptions were as predicted from the spectra of I and II (Table I, Figure 2). The rate constants were independent of wavelength, within experimental error (±2%). The important point is that the rate of loss of I is the same as the rate of formation

(6) Chattopadhyay, P. K.; Goetzee, J. F. *Anal. Chem.* **1972**, *44*, 2117.
(7) Coucouvanis, D.; Baenziger, N. C.; Kanatzidis, M. K., to be submitted.
(8) The Nujol mull of the complex was prepared in total darkness and the infrared spectrum was recorded in a totally dark instrument room. The possibility that cleavage of the C–C bond and formation of SCO is a thermal process was ruled out since samples preheated for 4 h to the temperature of the sample compartment (ca. 50 °C) did not show the 2055-cm^{-1} band in the first scan.
(9) Lathan, A. R.; Haskall, V. C.; Gray, H. B. *Inorg. Chem.* **1965**, *4*, 788.

Table II. Second-Order Rate Constants[a] for the Reaction between $(Bu_4N)_2Cu(Dto)_2$ and $(Bu_4N)FeCl_4$ in the Absence of Supporting Electrolyte in CH_2Cl_2

$10^4[(Bu_4N)$-$Fe_2Cl_4]_0$, M	$10^5[(Bu_4N)_2$-$Cu(Dto)_2]_0$, M	30 °C $10^{-5}k_{1f}$, M^{-1} s^{-1}	25 °C $10^{-4}k_{1f}$, M^{-1} s^{-1}	20 °C $10^{-4}k_{1f}$, M^{-1} s^{-1}	15 °C $10^{-4}k_{1f}$, M^{-1} s^{-1}
26.7	4.62	1.26 ± 0.03	9.55 ± 0.41	8.09 ± 0.49	6.85 ± 0.23
22.1	9.08	1.15 ± 0.01	9.86 ± 0.14	7.92 ± 0.13	6.92 ± 0.04
16.7	1.78	1.13 ± 0.07	9.26 ± 0.21	7.49 ± 0.29	6.23 ± 0.29
12.5	3.80	1.14 ± 0.05	9.20 ± 0.24	6.71 ± 0.24	5.83 ± 0.17
9.45	2.66	1.15 ± 0.02	9.56 ± 0.14	7.20 ± 0.36	5.57 ± 0.10
6.75	3.30	1.22 ± 0.05	10.10 ± 0.30	7.79 ± 0.20	6.71 ± 0.26
5.20	2.03	1.16 ± 0.09	8.96 ± 0.79		
18.3[b]	4.65[c]	(5.03 ± 0.20)	(4.11 ± 0.29)	(3.36 ± 0.13)	(2.93 ± 0.07)
		av[d] 1.17 ± 0.05	9.50 ± 0.40	7.53 ± 0.51	6.35 ± 0.56

[a] Measured at 430 nm. [b] $(BzPh_3P)FeCl_4$ used as the oxidant and measured at 435 nm. [c] $(BzPh_3P)_2Cu(Dto)_2$ complex used. [d] The average excludes the last entry. The uncertainties represent standard deviations from the mean for both individual rate constants and the averages.

Table III. Second-Order Rate Constants[a] for the Reaction between $(Bu_4N)_2Cu(Dto)_2$ and $(Bu_4N)FeCl_4$ with 0.1 M Bu_4NCl in CH_2Cl_2

$10^4[(Bu_4N)$-$Fe_2Cl_4]_0$, M	$10^5[(Bu_4N)_2$-$Cu(Dto)_2]_0$, M	30 °C $10^{-4}k_{1f}$, M^{-1} s^{-1}	25 °C $10^{-4}k_{1f}$, M^{-1} s^{-1}	20 °C $10^{-4}k_{1f}$, M^{-1} s^{-1}	15 °C $10^{-4}k_{1f}$, M^{-1} s^{-1}
26.1	4.48	7.70 ± 0.19	6.28 ± 0.23	5.21 ± 0.07	4.44 ± 0.15
23.0	2.54	7.57 ± 0.03	6.30 ± 0.09	5.39 ± 0.52	4.34 ± 0.02
19.9	2.03	7.99 ± 0.35	6.43 ± 0.30	5.13 ± 0.09	4.17 ± 0.21
15.9	6.85	7.92 ± 0.27	6.60 ± 0.13	5.67 ± 0.11	4.57 ± 0.12
10.0	3.55	7.98 ± 0.24	6.58 ± 0.20	5.51 ± 0.11	4.72 ± 0.18
7.30	2.79	8.34 ± 0.65	7.26 ± 0.28	6.00 ± 0.22	
2.32	1.27	8.70 ± 0.83	6.94 ± 0.49		
		av[b] 8.03 ± 0.38	6.62 ± 0.36	5.49 ± 0.32	4.45 ± 0.21

[a] Measured at 430 nm. [b] The uncertainties represent standard deviations from the mean for both the individual rate constants and the averages.

Table IV. Second-Order Rate Constants[a] for the Reaction between $(Bu_4N)_2Cu(Dto)_2$ and $(Bu_4N)_2CuCl_4$ with 0.1 M Bu_4NCl in CH_2Cl_2

$10^5[(Bu_4N)_2$-$CuCl_4]_0$, M	$10^5[(Bu_4N)_2$-$Cu(Dto)_2]_0$, M	30 °C $10^{-6}k_{1f}$ M^{-1} s^{-1}	25 °C $10^{-6}k_{1f}$ M^{-1} s^{-1}	20 °C $10^{-6}k_{1f}$ M^{-1} s^{-1}	15 °C $10^{-6}k_{1f}$ M^{-1} s^{-1}
19.4	1.52			1.01 ± 0.03	0.72 ± 0.02
14.0	0.90	1.81 ± 0.08	1.35 ± 0.15	1.03 ± 0.02	0.76 ± 0.08
11.2	0.76	1.51 ± 0.02	1.36 ± 0.02	0.89 ± 0.11	
9.20	0.75	1.68 ± 0.04	1.34 ± 0.05	0.97 ± 0.04	0.74 ± 0.02
7.70	0.90	1.56 ± 0.02	1.23 ± 0.03	0.81 ± 0.07	0.66 ± 0.01
		av[b] 1.64 ± 0.13	1.32 ± 0.06	0.94 ± 0.09	0.72 ± 0.04

[a] Measured at 380 nm. [b] The uncertainties represent standard deviations from the mean for both the individual rate constants and the averages.

of II. In general, individual kinetic experiments were carried out with an excess of oxidizing agent in order to maintain pseudo-first-order reaction conditions.

For the reaction systems consisting of the dithiooxalate complex I and iron(III), the disappearance of complex I was generally followed and a graph of $\ln (A_\infty - A_t)$ as a function of time was linear for more than 90% of the reaction.

The results of a detailed study of the reaction between $(Bu_4N)_2Cu(Dto)_2$ and $(Bu_4N)FeCl_4$ with 0.1 M Bu_4Cl are shown in Figure 3. The apparent rate constants (k_{obsd}) are a function of the initial concentration of the dithioxalate complex. The straight lines, obtained from graphs of the observed first-order rate constants (k_{obsd}) as a function of the initial concentration of iron(III), pass through the origin at zero concentration of initial complex, indicating that the rate of the back-reaction is very slow. These observations also rule out spontaneous reactions of the dithiooxalate complex.

From the kinetic data, which are consistent with the reaction

$$[Cu(Dto)_2]^{2-} \underset{k_{1d}\,(+e^-)}{\overset{k_{1f}\,(-e^-)}{\rightleftharpoons}} [Cu(Dto)_2]^-$$

the observed rate constant, k_{obsd}, can be rewritten as follows:

$$k_{obsd} = k_{1f}[Fe(III)]_0$$

A summary of the various second-order rate constants (k_{1f}) is shown in Tables II–IV.

The reaction between $(Bu_4N)_2Cu(Dto)_2$ and $(Bu_4N)_2CuCl_4$ in 0.1 M Bu_4NCl was also studied in detail by following the formation of complex II at 380 nm. The second-order rate constants (k_{1f}) are more than 10 times faster than the corresponding reaction using iron(III). A summary of the rates using $CuCl_4^{2-}$ is shown in Table IV. Due to the high rate of reaction, the concentrations of $CuCl_4^{2-}$ and $(Bu_4N)_2Cu(Dto)_2$ were kept within a small restricted range in order to maintain pseudo-first-order conditions.

Electrochemical Studies. The electrochemical oxidation of I occurs reversibly in CH_2Cl_2 at all scan rates studied (0.02–20 V/s). A typical set of cyclic voltammetric data is summarized in Table V. The $E_{1/2}$ ia +0.128 ± 0.003 V vs. SCE and the ΔE_p values are about 83 mV. While these values are larger than the theoretical value of 58 mV, they are similar to what has been observed in CH_2Cl_2 on this electrochemical system for known reversible processes. The measurement of accurate peak potentials is important in the analysis of the kinetic data. In order to reduce the effect of solution resistance on the results, the uncompensated resistance was electronically compensated for by positive feedback. To achieve a more effective compensation a stabilizing capacitor (500 pF) was placed between the auxiliary and reference electrodes.[10,11] The voltammetric wave of the known reversible oxidation of $[Ni(MNT)_2]^{2-}$[12] was examined to ensure that this

(10) Britz, D. *J. Electroanal. Chem.* **1978**, *88*, 309.
(11) Britz, D. *Electrochim. Acta* **1980**, *25*, 1449.

Table V. Cyclic Voltammetric Data

$(Ph_4P)_2Cu(S_2C_2O_2)_2$[a]

v, V/s	E_{pa}[b]	i_{pa}, μA	$i_{pa}/(v^{1/2}C)$[c]	E_{pc}[b]	i_{pc}/i_{pa}
0.020	0.176	7.5	49.1	0.090	0.48
0.050	0.175	10.6	43.9	0.085	0.73
0.100	0.165	14.9	43.6	0.092	0.89
0.200	0.170	20.8	43.1	0.085	0.94

$(Ph_4P)Cu(S_2C_2O_2)_2$[d]

v, V/s	E_{pc}	i_{pc}, μA	$i_{pc}/(v^{1/2}C)$	E_{pa}	i_{pa}/i_{pc}
0.020	0.101	4.9	41.2	0.175	0.60
0.050	0.105	7.6	40.5	0.161	0.82
0.10	0.103	11.0	41.4	0.167	0.90
0.20	0.101	15.4	41.0	0.165	0.93
0.50	0.100	24.8	41.8	0.175	0.92

[a] 1.08 mM $(Ph_4P)_2Cu(S_2C_2O_2)_2$, 0.11 M tetra-*n*-butylammonium perchlorate (TBAP), Pt electrode, 24 °C in CH_2Cl_2. [b] V vs. SCE. [c] μA $(V/s)^{-1/2}$ mM^{-1}; C = concentration of electroanalyte, mM. [d] 0.84 mM $(Ph_4P)Cu(S_2C_2O_2)_2$, 0.10 M TBAP, Pt electrode, 24 °C, in CH_2Cl_2.

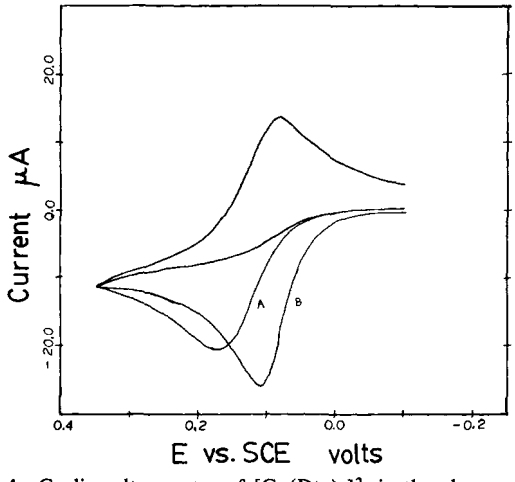

Figure 4. Cyclic voltammetry of $[Cu(Dto)_2]^{2-}$ in the absence (A) of triphenylphosphine and in the presence (B) of triphenylphosphine. (8.9 mM; v = 0.10 V/s).

capacitance did not cause any distortion in the shape of the wave. Although it has been shown previously[13,14] that this by-pass capacitor can enable more effective compensation without distortion, it was still difficult to achieve complete compensation. In any event, the peak potential separation values, ΔE_p, for the $[Cu(Dto)_2]^{2-/-}$ couple were no larger than those for the $[Ni(MNT)_2]^{2-/-}$ couple. The effects of uncompensated resistance were reduced further by comparing peak potentials at the same scan rates, where the small residual effect of solution resistance on the peak potentials is expected to cancel out. The product of the oxidation of I is stable on the voltammetric time scale, with peak current ratios (i_{pa}/i_{pc}) between 0.9 and 1.0 for all but the slowest scan rates, where convection becomes important. The average value for the current function[15] is 43.1 μA $(V/s)^{-1/2}$ mM^{-1} and agrees well with the known[16] value for one-electron diffusion-controlled processes.

The electrochemical reduction of II also is a reversible process over the same scan rates studied for I. The average half-wave potential ($E_{1/2}$) for II is +0.135 ± 0.002 V. The reduction of II (Table V) is again diffusion controlled, with I as the stable reduction product. The electrochemical redox process can be summarized as

$$[Cu(Dto)_2]^{2-} \rightleftarrows [Cu(Dto)_2]^{-} + e^{-}$$

Further evidence that II is the product of the oxidation of I is available in voltammetric studies of the oxidation of I in the presence of triphenylphosphine, PPh_3 (Figure 4). The formation of the $[Cu(Dto)(PPh_3)_2]^-$ complex[2] and the isolation of crystalline $(BzPh_3P)[Cu(Dto)(PPh_3)_2]$ can be accomplished readily (see Experimental Section) by the reaction $[Cu(Dto)_2]^- + 2PPh_3 \rightarrow [Cu(Dto)(PPh_3)_2]^- + 2COS$. In the presence of even low concentrations of triphenylphosphine, the cathodic wave disappears and the anodic peak potential shifts to more negative values (Figure 4). The shape of the oxidation wave (anodic peak) indicates a reversible process over a wide range of PPh_3 concentrations with $E_{pp/2}$ values ($E_p - E_{p/2}$) between 50 and 60 mV. The results for various PPh_3 concentrations are listed in Table VI and are consistent with a reversible oxidation of I to II followed by the irreversible reaction of II with PPh_3. The shift in the peak potential with scan rate and PPh_3 concentrations (Table VI) is predicted from the theory of a pseudo-first-order reaction following electron transfer.[15] The E_{pa} values (T = 25 °C) from Table VI

Table VI. Electrochemistry of $(Ph_4P)_2Cu(C_2S_2O_2)_2$ in the Presence of Triphenylphosphine[a]

$[Ph_3P]$, mM	v, V/s	E_{pa}[b]	$i_{pa}/(v^{1/2}C)$[c]	ΔE,[d] mV	k_f[e]
4.5	0.050	0.101	50.3	84	1.56
	0.10	0.111	48.9	74	1.38
	0.20	0.122	48.9	63	1.23
8.9	0.020	0.080	49.7	105	1.57
	0.050	0.096	48.9	89	1.16
	0.10	0.105	48.4	80	1.14
	0.20	0.112	46.5	73	1.31
19	0.020	0.075	50.8	110	1.11
	0.050	0.088	47.5	97	1.03
	0.10	0.095	46.9	90	1.15
	0.20	0.103	45.8	82	1.23
38.7	0.020	0.068	47.5	117	0.95
	0.050	0.077	46.8	108	1.16
	0.10	0.086	44.0	99	1.10
	0.20	0.097	44.7	88	0.96

[a] 0.064 mM $(Ph_4P)_2Cu(C_2S_2O_2)_2$, in methylene chloride, 0.105 M TBAP, 24 °C, Pt electrode. [b] V vs. SCE. [c] μA $(V/s)^{-1/2}$ mM^{-1} (C = concentration of $(Ph_4P)_2Cu(C_2S_2O_2)_2$, mM). [d] Shift in peak potential from when $[Ph_3P] = 0$. [e] $\times 10^{-5}$ M^{-1} s^{-1}.

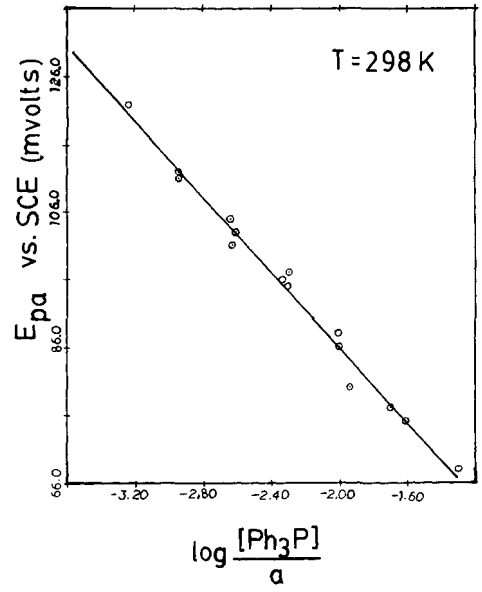

Figure 5. Variation in the E_{pa} values for $Cu(S_2C_2O_2)_2^{2-}$ as a function of log ($[Ph_3P]/a$) at 24 °C in the CH_2Cl_2.

(12) McCleverty, J. A. *Prog. Inorg. Chem.* **1968**, *10*, 49.
(13) Whitson, P. E.; Vandenborn, H. W.; Evans, D. H. *Anal. Chem.* **1973**, *45*, 1298.
(14) Brown, E. R.; Smith, D. E.; Booman, G. L. *Anal. Chem.* **1968**, *40*, 1411.
(15) Nicholson, R. S.; Shain, I. *Anal. Chem.* **1964**, *36*, 706.
(16) Very similar values of the current function are found for the known[12] electron oxidation of $[Ni(MNT)_2]^{2-}$. The latter is expected to have a diffusion coefficient very similar to that of $Cu(Dto)_2^{2-}$.

were plotted in Figure 5 as a function of log ($[PPh_3]/a$), where $a = nFv/RT$ and v is the scan rate. From the work of Nicholson and Shain[15] the relationship between E_{pa} and log ($[PPh_3]/a$) is given[17] by

$$E_{pa} = (E_{p,nr} - 8.5 - 29.5 \log k_f) - 29.5 \log ([PPh_3]/a)$$

where E_p,nr is the anodic peak potential with no triphenylphosphine present. The observed slope in Figure 5 was 28 mV, and from the intercept a rate constant of 1.3×10^5 M^{-1} s^{-1} can be calculated. A plot similar to the one shown in Figure 5 was obtained at a temperature of 2 °C and a rate constant of 4.8×10^3 M^{-1} s^{-1} was calculated. In this case the slope was 30 mV (compared to the theoretical value[15] of 27.2 mV at this temperature). The reaction also was studied at −43 °C and a rate constant of 6.2 M^{-1} s^{-1} was measured. Because the rate constant was small, the slope analysis could not be used. Instead, the rate constants were calculated directly from the table of Nicholson and Shain.[15] With admittedly limited data, the $\Delta H^{\ddagger}$ was calculated to be 13 ± 5 kcal/mol and the $\Delta S^{\ddagger}$ was 3.5 ± 3 cal/(mol K). In general, it is rather difficult to measure the electron-transfer rates for rapid processes because high scan rates must be used. In addition, in solvents such as CH_2Cl_2, high scan rates do not yield reliable data. One of the consequences of a rapid chemical reaction following electron transfer is that the anodic wave is shifted to more negative potentials. The shift in potential of the oxidation wave allows for an estimation of the lower limit for the heterogeneous electron transfer rate k_s because for the anodic process

$$\text{Red} - ne^- \underset{k_b}{\overset{k_{hf}}{\rightleftharpoons}} \text{Ox}$$

the forward electron-transfer rate, k_{hf}, is highly dependent upon the potential[18]

$$k_{hf} = k_s \exp[(E - E^\circ)(1 - \alpha)nF/RT]$$

(where α is the transfer coefficient). The wave eventually can be shifted into a potential region where k_{hf} is too small to maintain reversibility. When this occurs the wave will broaden and appear quasi-reversible and then irreversible. Furthermore, the E_{pa} value will be independent of the concentration of the reactant A in the reaction following electron transfer

$$\text{Ox} + \text{A} \xrightarrow{k_f} \text{product}$$

In the reaction

$$[Cu(Dto)_2]^{2-} - e^- \underset{k_b}{\overset{k_{hf}}{\rightleftharpoons}} [Cu(Dto)_2]^-$$

$$[Cu(Dto)_2]^- + 2Ph_3P \xrightarrow{k_f} [Cu(Dto)(PPh_3)_2]^- + 2COS$$

the anodic wave did not broaden significantly and continued to shift with added triphenylphosphine. However, at the highest concentration of Ph_3P used (88 mM) the wave did not shift as much as one would have expected based upon the concentration, and the calculated rate constant was less than the values obtained at the other concentrations. It appears then that the electron transfer itself is beginning to become rate limiting.

The limits under which the electron transfer will remain reversible even though the product of the oxidation is unstable have been determined by Nadjo and Saveant.[19] A calculation of the minimum value for k_s is possible considering the most extreme conditions where the electron transfer is still reversible. If the chemical reaction following electron transfer is fast enough to eliminate the reverse wave in the cyclic voltammogram, the following inequality must apply.[19]

$$\log p \geq 2.17$$

where $P = 2^{1/2}\Lambda^2\gamma^{-1/2}$, $\Lambda = k_s(Da)^{-1/2}$, $\lambda = [Ph_3P]k_f/a$, D is the diffusion coefficient, and $a = nFv/RT$. For the most extreme conditions[20] where the electron transfer is still reversible, i.e., the highest PPh_3 concentration (0.039 M) and the slowest scan rate ($v = 0.020$ V s^{-1}), $\lambda = 6510$ M^{-1} s^{-1}, Λ must be greater than 91 and k_s must be greater than 0.2 cm/s if $D = 8 \times 10^{-6}$ cm^2/s.[19] For k_s values smaller than 0.2 cm/s the wave would begin to appear quasi-reverisble (broader) and the shift of the anodic peak potential (E_{pa}) vs. scan rate would be significantly greater than 30 mV/log v.

A value for k_s of >0.2 cm/s reflects a very rapid electron-transfer rate and is about as fast as the rates observed with aromatic hydrocarbons (~0.6–5 cm/s)[21] or quinones (0.12–1.3 cm/s).[22]

The cyclic voltammetry of $FeCl_4^-$ and $CuCl_4^{2-}$ was studied in CH_2Cl_2 in order to measure the E° values. The reduction of $FeCl_4^-$ appears as a simple, one-electron quasi-reversible wave, with an E° value of +120 mV vs. SCE. The reduction of $CuCl_4^{2-}$ appears as a single very broad quasi-reversible wave with E_{pc}, ΔE_p, and $E_{pp/2}$ values of 270, 680, and 265 mV, respectively. The peak current function is about 50% above that for a one-electron process. The extreme broadness may be due to the overlap of the Cu^{II}/Cu^{I} and Cu^{I}/Cu^{0} waves. In any case the E° for the reduction is probably between +0.5 and +0.6 V and shows that $CuCl_4^{2-}$ is a stronger oxidizing agent than $FeCl_4^-$ under these conditions.

Discussion

Chemical and Electrochemical Kinetic Studies. The large difference between the second-order rate constants for the reaction of the dithiooxalate complex I with iron(III) and copper(II), respectively, suggests that the nature of the oxidant metal ion markedly affects the rate-determining step. Furthermore, these data rule out a first-order decomposition of I. The higher reaction rates of I with the $CuCl_4^{2-}$ oxidant, by comparison to corresponding rates with $FeCl_4^-$, are expected on the basis of the Marcus theory.[23] The cyclic voltammetric data show that under identical reaction conditions $CuCl_4^{2-}$ is a considerably stronger oxidant than $FeCl_4^-$.

The oxidation of I can be envisioned to proceed via a ternary complex where the oxidant (M^{n+} L_x) is complexed to the oxygen atoms of the coordinated dithiooxalate ligand. The propensity of the α-diketone end of the S,S'-coordinated dithiooxalate ligand toward coordination to Lewis acids is well-established[24] and is manifested in the coordination of the $[K(18\text{-crown-}6)]^+$ cation to the Dto ligands in the $[Cu(Dto)_2]^{2-}$ anion.[7] The very facile electrochemical oxidation of I on a platinum anode, however, shows that additional metal coordination to I is not necessary for electron transfer and the oxidation of I can be accounted for in terms of an outer-sphere mechanism without any bound intermediates. The heterogeneous electron-transfer rate that is observed electrochemically for the oxidation of I is among the fastest measured for inorganic molecules in nonaqueous solvents and is comparable to the heterogeneous electron-transfer rates k_s obtained in acetonitrile solution for the oxidation of certain Fe(II), Fe(III), and Mn(III) dithiocarbamate complexes.[25] In the latter complexes

(17) From ref 16: $E_{pc} = E_{1/2} - RT/nF$ (780 mV − ln $(k_f/a)^{1/2}$. Since $E_{1/2} = E_{p,nr} + 28$ mV, $E_{pc} = E_{pc,nr} + 28.5$ mV − 20 mV + 0.0257 ln $(k_f/a)^{1/2} = E_{pc,nr} + 8.5 + 29.5 \log k_f + 29.5 \log ([Ph_3P]/\alpha)$ and $E_{pa} = E_{pa,nr} - 8.5 - 29.5 \log k_f - 2.95 \log ([Ph_3P]/a)$.

(18) Bard, A. J.; Faulkner, L. R. "Electrochemical Methods: Fundamentals and Applications"; Wiley: New York, 1980.

(19) Nadjo, L.; Saveant, J. M. *J. Electroanal. Chem.* **1973**, *48*, 113. The area A of the Pt working electrode was determined with $K_4Fe(CN)_6$ as a standard with known diffusion coefficient $D = 1.183 \times 10^{-5}$ cm^2/s. The value of A (0.052 ± 0.015 cm^2) was used to calculate D for $(Ph_4P)_2Cu(Dto)_2$ over the range from 0.02 to 0.02 V/s. Using the formula $i = 602n^{3/2} A (Dv)^{1/2}C^*(\pi)^{1/2}\chi(\sigma t)$ we obtain the value of $D = (8.0 \pm 2.0) \times 10^{-6}$ cm^2/s.

(20) The linearity of the E_{pa} vs. log ($[Ph_3P]/a$) plot (Figure 5) shows that the electrochemical reaction is still reversible at Ph_3P concentrations as large as 0.039 M. In addition, the wave shape ($E_{pp/2}$) values and the $\Delta E_{pa}/\Delta(\log v)$ values do not change up to a PPh_3 concentration of 0.039 M. The choice of the "highest" PPh_3 concentration (0.039 M) therefore is justified on the basis that it takes into account the entire wave.

(21) Kojima, H. K.; Bard, A. J. *J. Am. Chem. Soc.* **1975**, *97*, 6317.

(22) Rosanke, T. W.; Evans, D. H. *J. Electroanal. Chem.* **1976**, *72*, 277.

(23) Marcus, R. A. *J. Phys. Chem.* **1963**, *67*, 853.

(24) Coucouvanis, D. "Verlag für Chemie, Transition Metal Chemistry"; Müller, A., Diemann, E., Eds.; 1981 p 59.

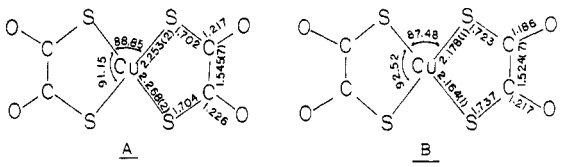

Figure 6. Structure of the $Cu(Dto)_2^{n-}$ (n = 1, 2) anions:[7] (A) n = 2; (B) n = 1.

Table VII. Activation Parameters for the Oxidation of the $Cu(Dto)_2^{2-}$ Complex

reaction system	$\Delta S^{\ddagger}$	$\Delta H^{\ddagger}$
$(Bu_4N)_2Cu(Dto)_2$-$(Bu_4N)FeCl_4$	−13.7 ± 1.21	6.59 ± 0.36
$(Bu_4N)_2Cu(Dto)_2$-$(Bu_4N)FeCl_4$-0.1 M Bu_4NCl	−16.3 ± 0.03	6.00 ± 0.09
$(BzPh_3P)_2Cu(Dto)_2$-$(BzPh_3P)FeCl_4$	−18.2 ± 1.60	5.74 ± 0.46
$(Bu_4N)_2Cu(Dto)_2$-$(Bu_4N)_2CuCl_4$-0.1 M Bu_4NCl	0.15 ± 1.70	9.16 ± 0.50

these rates are in the range from 0.1 to 2.0 cm/s, and, since there exist no pronounced ligand or structural changes following electron transfer, the rates must be controlled primarily by the reorganization of the inner solvation spheres. The value of k_s has been reported for the reduction of cyclooctatetraene.[26] In this case a conformational change from the "tub" to the planar configuration occurs upon reduction and k_s is 2.0×10^{-3} cm/s.

Considering the available data on heterogeneous electron-transfer rates and comparing these data to the k_s for the oxidation of I, it becomes apparent that in the chemical oxidation of I by either Fe(III) or Cu(II) the electron transfer is rate determining and the activation parameters that are calculated (Table VII) are related to the electron-transfer step.

The facile photolysis of II is not without precedent in the chemistry of metal complexes with sulfur ligands. The $[Fe^{IV}(Et_2Dtc)_3]^+$ complex is reported[27] to undergo an intramolecular charge transfer to the metal accompanied by ligand oxidation:

$$[Fe^{IV}(Et_2Dtc)_3]^+ \xrightarrow{h\nu} [Fe^{II}(Et_2Dtc)_2\cdots Et_2Dtc^+]^*$$

$$[Fe^{II}(Et_2Dtc)_2\cdots Et_2Dtc^+]^* \rightarrow Fe^{II}(Et_2Dtc)_2 + Et_2Dtc^+$$

A similar type of photolytic behavior very likely occurs with II and results in the oxidative C–C bond cleavage of the Dto ligand. The Dto–Cu charge transfer is promoted by PPh_3 and results in the cleavage of the C–C bond even in the absence of light. The exact mechanism of interaction between II and PPh_3 is difficult to ascertain. However, whether it occurs by an associative or a dissociative pre-electron-transfer step it must involve an intermediate with an electronic structure that has the unoccupied copper $d_{x^2-y^2}$ orbital close in energy to a symmetry-compatible bonding orbital of the Dto ligand.

The photolytic behavior of II may not be unique and suggest that similar behavior could be occurring with other Cu(III) complexes. Photochemically induced intramolecular electron transfer may result in very short lifetimes for Cu(III) complexes which have been proposed as intermediates in redox reactions. An examination of such redox reactions in the absence of light may allow for the possible detection or isolation of light-sensitive Cu(III) intermediates. The presence of Cu(III) has been suggested[28] as possible in the active form of galactose oxidase. For this enzyme, which contains copper in the active site, sulfur coordination has been implicated[29] for the immediate copper coordination environment.

The facile, light-activated, intramolecular electron transfer in II and cleavage of the C–C bond in the coordinated Dto ligand is not evident in unusual structural characteristics of the $[Cu(Dto)_2]^{n-}$ anions. In the structures of the anions I and II (Figure 6) the C–C bond lengths of the Dto ligands at 1.545 (7) and 1.524 (7) Å, respectively,[7] are similar and are within 3σ from the "single" ($C(sp^3)$–$C(sp^3)$) bond length of 1.537 Å.[30]

Acknowledgment. This work has been generously supported by a grant from the National Institutes of Health (No. GM-18144-03).

Registry No. I, 46145-05-5; $I(Ph_4P)_2$, 88326-17-4; $I(Bu_4N)_2$, 88326-19-6; $I(BzPh_3P)_2$, 38999-75-6; $I(EtPh_3P)_2$, 88326-20-9; II, 88326-16-3; $(Bu_4N)Cu(Dto)$, 88326-22-1; $(BzPh_3P)Cu(Dto)$, 88326-23-2; $(EtPh_3P)Cu(Dto)$, 88326-24-3; $(Bu_4N)FeCl_4$, 23329-97-7; $(Bu_4N)_2CUCl_4$, 88326-18-5; $(BzPh_3P)FeCl_4$, 36021-10-0; Ph_3P, 603-35-0; Cu, 7440-50-8; Fe, 7439-89-6.

(25) Yasuda, H.; Suga, K.; Aoyagui, S. *J. Electroanal. Chem.* **1978**, *86*, 259.
(26) Huebert, B. J.; Smith, D. E. *J. Electroanal. Chem.* **1971**, *31*, 333.
(27) Miessler, G. L.; Zoebisch, E.; Pignolet, L. H. *Inorg. Chem.* **1978**, *17*, 3636.
(28) Hamilton, G. A.; Libby, R. D.; Hartzell, C. R. *Biochem. Biophys. Res. Commun.* **1973**, *55*, 333.
(29) Cleveland, L.; Coffman, R. E.; Coon, P.; Davis, L. *Biochemistry* **1975**, *14*, 1108.
(30) Tables of interatomic distances and configurations in molecules and ions. The Chemical Society: London, 1960.